J Therm Anal Calorim (2010) 102:75–81
DOI 10.1007/s10973-010-0773-1

BSA denaturation in the absence and the presence of urea studied by the iso-conversional method and the master plots method

Xiaomin Cao · Yun Tian · Zhiyong Wang · Yuwen Liu · Cunxin Wang

Received: 6 September 2009 / Accepted: 24 March 2010 / Published online: 10 April 2010

Abstract The kinetics of bovine serum albumin (BSA) denaturation in the absence and the presence of urea was studied by the iso-conversional method and the master plots method using differential scanning calorimetry (DSC). The observed denaturation process was irreversible and approximately conformed to the simple order reaction, and the denaturation did not follow rigorously first-order kinetic model or other integral order reaction models. The denaturation temperature (T_m), apparent activation energy (E_a), approximate order of reaction (n), and pre-exponential factor (A) all distinctly decreased as the 2 mol L^{-1} urea was added, which indicated that the urea accelerated the denaturation process of BSA and greatly reduced thermal and kinetic stability of BSA. This study also demonstrated that the iso-conversional method, in combination with the master plots method, provides a valuable and useful approach to the study of the kinetic process of protein denaturation.

Keywords BSA · Urea · DSC · Denaturation · The iso-conversional method and the master plots method

X. Cao (✉)
Changsha Environmental Protection College, ChangSha 410004, Hunan, China
e-mail: caograss2003@yahoo.com.cn

Y. Tian
Environmental Monitoring Center of Hunan Province, ChangSha 410014, Hunan, China

Z. Wang · Y. Liu · C. Wang
College of Chemistry and Molecular Science, Wuhan University, Wuhan 430072, Hubei, China

Introduction

The denaturation of proteins is, in general, triggered by a conformational change of the protein induced by heat, adding denaturants, or other processes that affect the folded structure. Bovine serum albumin(BSA), molecular mass 66500 Da, is built from 583 amino acid residues containing 20 Tyr. with well-characterized physiochemical properties [1–3]. Differential scanning calorimetry (DSC) is widely used for the study of thermal protein denaturation. Although extensive literatures have been published on the experimental and theoretical aspects of BSA denaturation [4–11] based on the Lumry–Eyring model [12] by DSC,report on the kinetic aspect of the BSA denaturation process using the iso-conversional and the master plots method is rarely available in literature [13]. Model-free approaches represented by iso-conversional method to give excellent results of dependencies of the activation energy on the extent of conversion of nonisothermal experiments. The analysis of the activation energy dependency will provide important clues on reaction mechanism [14–17], and the master plots method will give more insight into the mechanism of denaturation process.

Urea is a frequently used protein denaturant. It has affinity with hydrophobic side chains and peptide groups, and can disrupt the three-dimensional structure of proteins and denatures them. The denaturation of protein in the presence of urea has been exhaustively studied [18–24], however, the kinetic aspect of the denaturation process for BSA may not be explicit. The combination of iso-conversional method and the master plots method might provide new opportunities in exploring the kinetic process of protein denaturation. In this contribution, the denaturation kinetics of BSA in the absence and the presence of urea was investigated by the iso-conversional method and the master plots method using DSC.

Theoretical approach

The theory refers to the literature reported by Tang et al. [25], and the detailed explanation refers to our previous reports [26–28]. For a reaction under non-isothermal condition, its kinetic function can be described in the following form:

$$g(\alpha) = \frac{AE_a}{\beta R} P(u) \tag{1}$$

where α is the extent of conversion (in order to obtain α (conversion of reaction), the following equations are used: in DSC, $\alpha = \frac{\Delta H_{part}}{\Delta H_{tot}}$, ΔH_{part} is partial area [J g^{-1}] and ΔH_{tot} is total peak area [J g^{-1}]), β is the heating rate, E_a is the apparent activation energy, R is the gas constant, A is pre-exponential factor, $g(\alpha)$ is the integral expression of kinetic model function, and $P(u) = \int_{\infty}^{u} -(e^{-u}/u^2)du$, $u = E_a/RT$. Because the exponential integral, $P(u)$, has no analytical solution, an approximate formula of high accuracy, which is directly obtained from numerical integration of temperature integral without derivation from any approximating infinite series [29, 30], was used.

$$P(u) = \exp(-u)/[u(1.00198882u + 1.87391198)] \tag{2}$$

Inserting Eq. 2 into Eq. 1, one can obtain:

$$\ln\left(\frac{\beta}{T^{1.894661}}\right) = \ln\left[\frac{AE_a}{Rg(\alpha)}\right] + 3.635041 - 1.894661 \ln E_a - 1.001450\frac{E_a}{RT} \tag{3}$$

The first term at the right side of Eq. 3 is a constant corresponding to a given value of α. Therefore, for a series of experiments at different heating rates, the plot of $\ln(\beta/T^{1.89466100})$ versus $1/T$ with the same conversional ratio should be a line with the slope of $-1.00145033E_a/R$. Then, the apparent activation energy E_a can be calculated from the slope. Inserting $\alpha = 0.5$ into Eq. 1, one can get:

$$g(0.5) = \frac{AE_a}{\beta R} P(0.5) \tag{4}$$

where $u_{0.5} = E_a/RT_{(0.5)}$. When Eq. 1 is divided by Eq. 4, the following equation is obtained:

$$\frac{g(\alpha)}{g(0.5)} = \frac{P(u)}{P(u_{0.5})} \tag{5}$$

By plotting $g(\alpha)/g(0.5)$ against α according to different theoretical model functions, the theoretical master plots can be obtained, for different kinetic mechanisms. With E_a calculated from Eq. 3, the experimental master plots of $P(u)/P(u_{0.5})$ against α could be drawn from the experimental data obtained under different heating rates. Equation 5 indicates that, for arbitrary α, the experimental value of $P(u)/P(u_{0.5})$ and theoretically calculated values of $g(\alpha)/g(0.5)$ are equivalent when an appropriate kinetic model is used. The integral master plots method can be used to determine the reaction kinetic models of non-isothermal reactions. Then, the pre-exponential factor A can be estimated from the slope of the plot of $g(\alpha)$ versus E_a $P(u)/\beta R$.

Experimental

Instruments and materials

Mettler Toledo calorimeter, model DSC 822^e (Switzerland); BSA (Fraction V, purity > 99.9%, Roche Chemical Company) was used without further purification. Distilled and deionized water was used for the preparation of all solutions. The 30 mg mL^{-1} BSA solution was prepared by dispersing powdered protein into 150 mol L^{-1} NaCl solution in the absence and the presence of 2 mol L^{-1} urea and stirring for at least 2 h.

Differential scanning calorimetry (DSC)

The protein solution (80 μL) was placed in 100-μL medium pressure crucible, and the corresponding buffer was used as reference. The instrument was calibrated with indium. Scanning calorimetry was performed with the Star® evaluation program, at different heating rates of 1.0, 1.5, 2.0, and 2.5 K min^{-1}, in the temperature range of 35–95 °C. After the end of the first heating round, the protein sample was quickly cooled to 35 °C, and rescanned after 5 min stabilization time at 35 °C. The sample is heated at a low heating rate (<2.5 K min^{-1}) to avoid thermal interference due to circulating convection currents in the sample vessel [31]. Measurements were carried out on two or three separate samples (replicates) and reported as the average. The peak temperature of the transition (T_m) was determined graphically in each case. The conversion (α) was calculated using the Star® software [32].

Results and discussion

DSC curves for 30 mg mL^{-1} BSA denaturation at different scan rates in the absence and the presence of urea are given in Figs. 1 and 2, respectively. The corresponding T_m was also displayed in Table 1. A different measurement was obtained by completing two sequential scans for a single sample. The first scan of the protein in the absence and the presence of urea exhibited only one endothermic transition between 65–87 and 57–82 °C as shown in Figs. 1 and 2, respectively. The observed denaturation process of BSA was always calorimetrically irreversible since no thermal

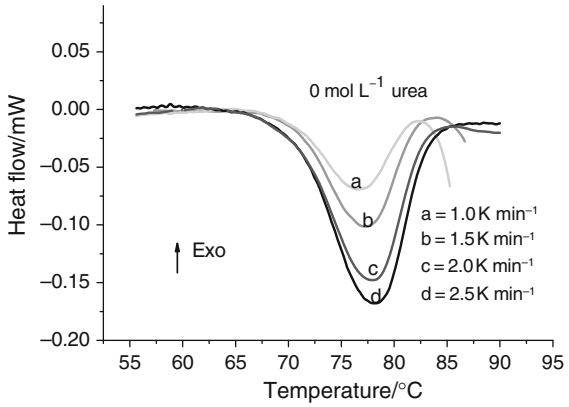

Fig. 1 DSC curves for 30 mg mL^{-1} BSA denaturation in the absence of urea at different heating rates

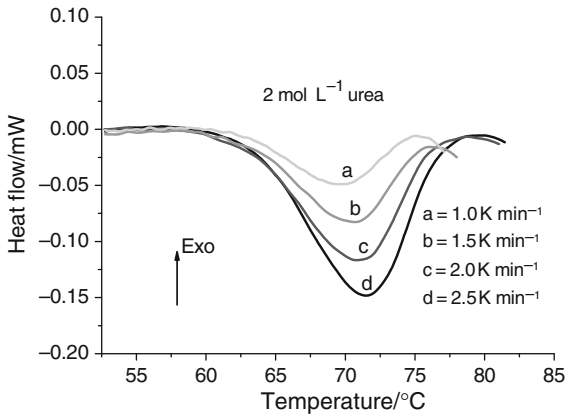

Fig. 2 DSC curves for 30 mg mL^{-1} BSA denaturation in the presence of urea at different heating rates

effect was observed for the second heating scan of the protein. The conclusion was supported by our subsequent result that the protein samples extracted from the calorimetric cell after the first heat scan showed a strong gelation state, which meant that irreversible denaturated aggregation occurred. BSA denaturation is irreversible probably due to the occurrence of "side" processes such as aggregation [33]. Owing to denaturation, hydrophobic interaction can occur, and exposed thiol groups can form disulfide bonds, which result in an irreversible behavior [34, 35].

NaCl can increase the thermal stability of BSA [36]. The increase of thermal stability can be explained by a reduction of inter-molecular electrostatic repulsion leading to a growth in the association of native molecules [37]. Identical increase in thermal stability has also been observed for *β*-lactoglobulin [37, 38], and for flaxseed (*Linum usitatissimum*) proteins [39].

As is evident in Figs. 1 and 2, T_m is highly dependent on scan rate. With decreasing scan rate, T_m decreases. It distinctly revealed that the scan rate substantially affected BSA denaturation. The highly dependent of T_m on the scan rate indicated that the denaturation process was, at least in part, under kinetic control.

As shown in Fig. 2, the urea exerted obvious influence on the BSA thermal denaturation. When the DSC curves in Fig. 1 were compared with the ones in Fig. 2, it is indicative that the T_m of BSA distinctly moved to low temperature direction as 2 mol L^{-1} urea was added at the same scan rate just as shown in Table 1. This illuminated that the urea accelerated the denaturation process of BSA and reduced the thermal stability of it.

The biological activity of proteins depends on their threedimensional structure, which is closely connected to hydration. It is generally believed that the conformational stability of most proteins results from a combination of conflicting effects: hydrophobicity and hydrogen bonding [40]. Urea alters the structure of BSA. The experimental results [41] showed that the interactions between protein and urea molecules mainly formed a hydrogen-bonding effect, and the inference could be drawn that the interaction should be a combination of multiple forms of hydrogen bonding, and this combination is more stable than the one of the single hydrogen bonding [42]. Urea destabilizes proteins by destroying the hydrogen bond which weakens the hydrophobic interactions between non-polar residues of proteins [43]. The collapse of the hydrogen bonding results in weaker hydrophobic interaction in the core of the globular proteins, thus causing faster protein denaturation [44].

Table 1 T_m of 30 mg mL^{-1} BSA in the absence and the presence of urea at different heating rates

Scanning rate/K min^{-1}	1	1.5	2	2.5
T_m/ °C				
Urea content/mol L^{-1}				
0	76.69 ± 0.06[a]	77.45 ± 0.03	77.97 ± 0.09	78.30 ± 0.12
2	69.40 ± 0.09	70.26 ± 0.07	70.93 ± 0.12	71.52 ± 0.11

[a] Means ± standard deviations

Standard deviations $S = \sqrt{\sum (X - M)^2/(n-1)}$

where Σ = Sum of, X = Individual score, M = Mean of all scores, n = Sample size (number of scores)

Non-isothermal kinetics for the denaturation of BSA in the absence and the presence of urea

Iso-conversional method for estimating activation energy dependence

Using the α–T data obtained from DSC conversion plots, according to corresponding Eq. 3, the apparent activation energy (E_a) of 30 mg mL^{-1} BSA denaturation in the absence of urea was estimated from the iso-conversional plot of $\ln(\beta/T^{1.894661})$ versus $1/T$ at different conversion ratios (α) in the range of 0.2–0.8. As shown in Fig. 3, the value of activation energy hardly varies with the degree of conversion. All these plots have linear correlation coefficients larger than 0.9950. It is worth mentioning that the average value of E_a is 550.38± 23.00 kJ mol^{-1}. This is comparable to the activation energy found for other proteins, such as, β-lactoglobulin [45], wild-type nitrite reductase [46], bovine fibrinogen [47], muscle creatine kinase [48], etc. The large value of E_a might be expected, because the highly cooperative nature of the protein implies a large $\triangle H$ between the folded and denatured protein, and E_a is always larger than ΔH [10, 49]. Owing to the little dependence of the activation energy on the extent of conversion, a simple reaction mechanism could be used for reaction progressing. Aggregation was probably one of the main causes of irreversibility in the transitions of BSA. Therefore, the inactivation kinetics might be expected to have a higher than one reaction order [50].

Master-plots method for determining kinetic model

In order to determine the most possible mechanism, 18 basic model functions listed in Table 2 were tested.

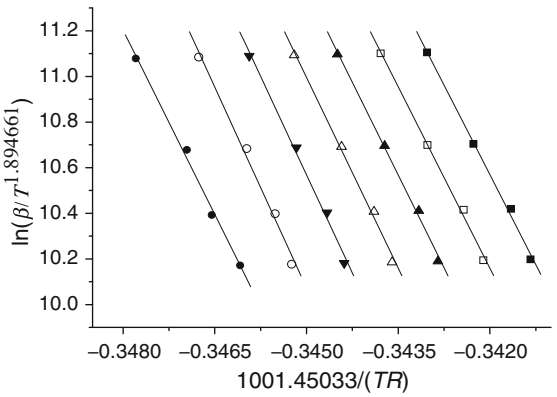

Fig. 3 Plots for determination of activation energy of 30 mg mL^{-1} BSA denaturation in the absence of urea at different α: 0.2 (*filled square*), 0.3 (*open square*), 0.4 (*filled triangle*), 0.5 (*open triangle*), 0.6 (*inverted filled triangle*), 0.7 (*open circle*), and 0.8 (*filled circle*). *Solid lines* are linear fitting corresponding to different α

According to the value of E_a, the theoretical master plots of $G(\alpha)/G(0.5)$ versus α and the experimental master plots of $P(u)/P(u_{0.5})$ versus α are obtained, as shown in Fig. 4. The

Table 2 The 18 model functions for the determination of the most probably model function

No.	Reaction model	Symbol	$G(\alpha)$
1	Avrami–Erofeyev, $m = 4$	A_4	$[-\ln(1-\alpha)]^{1/4}$
2	Avrami–Erofeyev, $m = 3$	A_3	$[-\ln(1-\alpha)]^{1/3}$
3	Avrami–Erofeyev, $m = 2$	A_2	$[-\ln(1-\alpha)]^{1/2}$
4	Avrami–Erofeyev, $m = 1.5$	$A_{1.5}$	$[-\ln(1-\alpha)]^{2/3}$
5	Phase boundary reaction, $n = 1$	R_1	α
6	phase boundary reaction, $n = 2$	R_2	$1-(1-\alpha)^{1/2}$
7	Phase boundary reaction, $n = 3$	R_3	$1-(1-\alpha)^{1/3}$
8	One-dimensional diffusion	D_1	$1/2\alpha^2$
9	Two-dimensional diffusion	D_2	$1/2[1-(1-\alpha)^{1/2}]^{1/2}$
10	Three-dimensional diffusion	D_4	$1-2\alpha/3-(1-\alpha)^{2/3}$
11	Jander's type diffusion	D_3	$[1-(1-\alpha)^{1/3}]^2$
12	Power law, $n = 1/4$		$\alpha^{1/4}$
13	Power law, $n = 1/3$		$\alpha^{1/3}$
14	Power law, $n = 1/2$		$\alpha^{1/2}$
15	Power law, $n = 3/2$		$\alpha^{3/2}$
16	First order	A_1, F_1	$-\ln(1-\alpha)$
17	Second order	F_2	$(1-\alpha)^{-1}-1$
18	Third order	F_3	$1/2[(1-\alpha)^{-2}-1]$

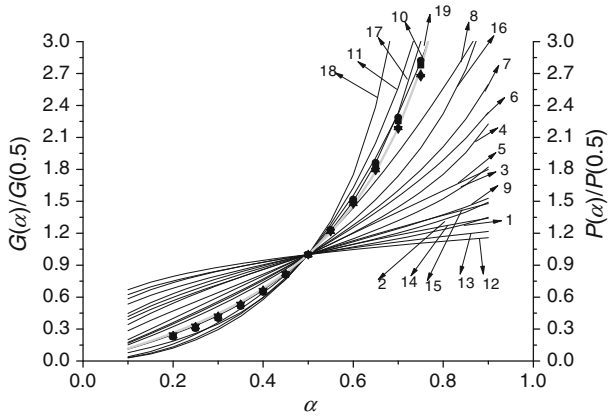

Fig. 4 Master plots of theoretical $P(u)/P(u_{0.5})$ against α for various reaction models (*solid curves*, as enumerated in Table 3, and curve 19 represents function $G(\alpha) = \frac{1}{1-1.80} - \frac{(1-\alpha)^{1-1.80}}{1-1.80}$) and experimental data for the BSA denaturation in the absence of urea at heating rates 1.0 K min^{-1} (*filled triangle*), 1.5 K min^{-1} (*inverted filled triangle*), 2.0 K min^{-1} (*filled square*), and 2.5 K min^{-1} (*filled circle*). Models that have been used to describe the simple order reaction process are labeled as: (16) first order reaction model; (17) second order reaction model; (18) third order reaction model

superposition of experiment master plotted at different heating rates indicated that the kinetics process of denaturation of the BSA in the absence of urea could be described by a single model function. From Fig. 4, the kinetic process is most probably described by F_n model,

$$G(\alpha) = \frac{1}{1-n} - \frac{(1-\alpha)^{1-n}}{1-n}$$

Because the experimental master plots lay between the theoretical master plots F_1 and F_2, it was likely that the apparent mechanism of overall reaction could not be expressed in terms of an integral order reaction model, which maybe indicated by mixture of basic reactions involved in the system.

Evaluation of pre-exponential factor and kinetic exponent

The kinetic exponent and pre-exponential factors were determined by further calculations. The expression of F_n was introduced into Eq. 1, and Eq. 6 was obtained

$$\frac{1}{1-n} - \frac{(1-\alpha)^{1-n}}{1-n} = \frac{AE_a}{\beta R}P(u) \quad (6)$$

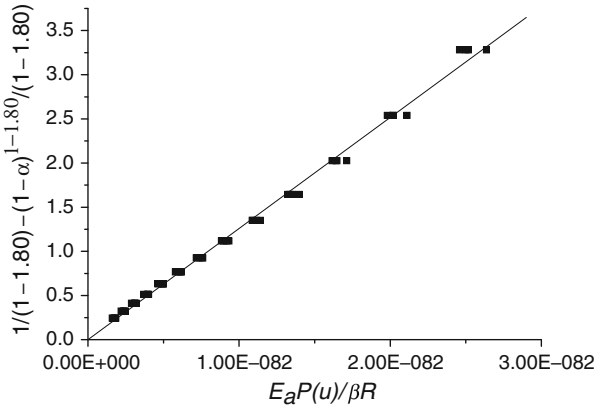

Fig. 5 Plotting $\frac{1}{1-n} - \frac{(1-\alpha)^{1-n}}{1-n}$ vs. $\frac{E_a}{\beta R}P(u)$ at $n = 1.80$ for BSA denaturation in the absence of urea at various heating rates and their linear-fitting drawing (*solid line*)

In Eq. 6, $P(u)$ could be calculated according to Eq. 2. Plotting $\frac{1}{1-n} - \frac{(1-\alpha)^{1-n}}{1-n}$ versus $\frac{E_a}{\beta R}P(u)$ from $n = 1$ to 2 with a step of 0.01, a series of straight lines through zero were obtained. The most reasonable exponent n was the one with the highest linear correlation coefficient. Our calculation showed that $n = 1.80$ led to the highest linear correlation coefficient of 0.99812 with $A = 1.26\text{E}82\ \text{s}^{-1}$ obtained from the slope of the line. The plots of $\frac{1}{1-n} - \frac{(1-\alpha)^{1-n}}{1-n}$ versus $\frac{E_a}{\beta R}P(u)$ at $n = 1.80$ at various heating rates, and their linear-fittings drawn through the zero point are shown in Fig. 5, respectively. All the apparent kinetic parameters that were determined during the main stage of BSA denaturation are summarized in Table 3. The class of kinetic models, F_n, can describe the observed denaturation process of BSA in the absence of urea.

Kinetic triplets for BSA denaturation in the presence of urea

The same procedures were repeated for the BSA denaturation in the presence of urea (2 mol L^{-1}). The activation energies were nearly independent of conversion and the mean activation energy was $430.77 \pm 10.42\ \text{kJ mol}^{-1}$. The presence of 2 mol L^{-1} urea evidently decreased the activation energy. Further calculations indicated that the class of kinetic models, F_n, best described the BSA denaturation in the presence of urea. The logarithmic value of pre-exponential factors and kinetic exponent are also presented in Table 3. The possible mechanisms for the BSA denaturation in the presence and the absence of urea, are simple order reactions. Compared with an idealized Avrami–Erofeyev equation, a nonintegral value of kinetic exponent n is more appropriate to describe the actual process. The activation energy (E_a), the approximate order of reaction (n), the pre-exponential factor (A) of the denaturation transition, and the denaturation temperature (T_m) decreased when the 2 mol L^{-1} urea was added (Tables 1 and 3). This suggested that the urea affected BSA denaturation substantially and decreased kinetic and thermal stability of BSA.

Table 3 Kinetic model and parameters for the BSA denaturation in the absence and the presence of urea

Urea content/mol L^{-1}	E_a/kJ mol^{-1}	A/s^{-1}	n	r	$G(\alpha)$
0	550.38 ± 23.00[a]	1.26E82	1.80	0.99812	$\frac{1}{1-1.80} - \frac{(1-\alpha)^{1.80}}{1-1.80}$
2	430.77 ± 10.42	2.35E65	1.36	0.99818	$\frac{1}{1-1.36} - \frac{(1-\alpha)^{1.36}}{1-1.36}$

[a] Means ± standard deviations

Standard deviations $S = \sqrt{\sum (X-M)^2/(n-1)}$

where Σ = Sum of, X = Individual score, M = Mean of all scores, n = Sample size (number of scores)

Conclusions

The study has shown that the denaturation of BSA in the absence and presence of urea was found calorimetrically irreversible as reflected by the lack of transition in the second run of all the samples. Little dependence of the apparent activation energy on the extent of conversion for the BSA denaturation in the absence and presence of urea indicated that a simple reaction mechanism with reaction progressing could be used. The most possible kinetic model was determined by using the master plots method, which indicated that the kinetic model might be described by an accommodated Avrami–Erofeyev equation, $G(\alpha) = \frac{1}{1-n} - \frac{(1-\alpha)^{1-n}}{1-n}$. The observed BSA denaturation studied in this article did not follow rigorously first-order kinetic model or other integral order reaction models. The DSC results on T_m and nonisothermal kinetics analysis of the BSA denaturation indicated that urea accelerated the denaturation process of BSA and reduced thermal and kinetic stability of BSA. This study represented the combination of iso-conversional method and the master plots method opened a new avenue in investigating in exploring the kinetics process of protein denaturation.

Acknowledgements This study was financially supported by the National Natural Science Foundation of China (Grant Nos. 20373050 and 30600116), the Natural Science Foundation of Hubei, and China Postdoctoral Science Foundation.

References

1. Murayama K, Tomida M. Heat-induced secondary structure and conformation change of bovine serum albumin investigated by Fourier transform infrared spectroscopy. Biochemistry. 2004;43: 11526–32.
2. Kinsella JE, Whitehead DM. Proteins in whey: chemical, physical and functional properties. Adv Food Nutr Res. 1989;33:343–8.
3. Peters TJ. All about albumin biochemistry, genetics and medical applications. San Diego, CA: Academic Press; 1996.
4. Feil WP, Privalov PL. Thermodynamic investigations of proteins: II. Calorimetric study of lysozyme denaturation by guanidine hydrochloride. Biophys Chem. 1976;4:33–40.
5. Gekko K, Ito H. Competing solvent effects of polyols and guanidine hydrochloride on protein stability. Biochem J. 1990;107: 572–7.
6. Conejero-Lara F, Sánchez-Ruiz JM, Mateo PL, Burgos FJ, Vendrell J, Avilés FX. Differential scanning calorimetric study of carboxypeptidase B, procarboxypeptidase B and its globular activation domain. Eur J Biochem. 1991;200:663–70.
7. Charman SA, Mason KL, Charman WN. Techniques for assessing the effects of pharmaceutical excipients on the aggregation of porcine growth hormone. Pharm Res. 1993;10:954–62.
8. Martínez JC, Filimonov VV, Mateo PL, Schreiber G, Fersht AL. A calorimetric study of the thermal stability of barstar and its interaction with barnase. Biochemistry. 1995;34:5224–33.
9. Funahashi J, Takamo K, Ogosahara K, Yamagata Y, Yutani K. The structure, stability, and folding process of amyloidogenic mutant human lysozyme. J Biochem. 1996;120:1216–23.
10. Weijers M, Barneveld PA, Stuart MAC, Visschers RW. Heat-induced denaturation and aggregation of ovalbumin at neutral pH described by irreversible first-order kinetics. Protein Sci. 2003; 12:2693–703.
11. Baier S, McClements DJ. Impact of preferential interactions on thermal stability and gelation of bovine serum albumin in aqueous sucrose solutions. J Agric Food Chem. 2001;49:2600–8.
12. Lumry R, Eyring H. Conformation changes of proteins. J Phys Chem. 1954;58:110–20.
13. Vyazovkin S, Vincent L, Sbirrazzuoli N. Thermal denaturation of collagen analyzed by isoconversional method. Macromol Biosci. 2007;7:1181–6.
14. Vyazovkin S, Wight CA. Isothermal and nonisothermal reaction kinetics in solids: in search of ways toward consensus. J Phys Chem A. 1997;101:8279–84.
15. Vyazovkin S, Wight CA. Model free and model fitting approaches to kinetic analysis of isothermal and non-isothermal data. Thermochim Acta. 1999;340:53–68.
16. Vyazovkin S. Kinetic analysis of reversible thermal decomposition of solids. Intl J Chem Kinet. 1995;27:73–84.
17. Vyazovkin S. A unified approach to kinetic processing of nonisothermal data. Intl J Chem Kinet. 1996;28:95–101.
18. Pace CN, Show KI. Linear extrapolation method of analyzing solvent denaturation curves. Proteins. 2000;41:1–7.
19. Vanzi F, Madan B, Sharp K. Effect of the protein denaturants urea and guanidinium on water structure: a structure and thermodynamic study. J Am Chem Soc. 1998;120:10748–53.
20. Makhatadze GI. Thermodynamics of protein interactions with urea and guanidinium hydrochloride. J Phys Chem. 1999;103: 4781–6.
21. Shimizu S, Chan HS. Origins of protein denatured state compactness and hydrophobic clustering in aqueous urea: inferences from nonpolar potentials of mean force. Proteins. 2002;49:560–6.
22. Wallqvist A, Covell DG, Thirumalai D. Hydrophobic interactions in aqueous urea solutions with implications for the mechanism of protein denaturation. J Am Chem Soc. 1998;120:427–8.
23. Chatterjee S, Basumallick I. Thermodynamic studies on amino acid solvation in aqueous urea. J Chin Chem Soc. 2007;54: 667–72.
24. Chatterjee S, Basumallick I. Transfer thermodynamics of protein in denaturing and stabilizing media. J Chin Chem Soc. 2008;55: 17–22.
25. Tang WJ, Wang CX, Chen DH. An investigation of the pyrolysis kinetics of some aliphatic amino acids. J Anal Appl Pyrolysis. 2006;75:49–53.
26. Cao XM, Li J, Yang X, Duan Y, Liu YW, Wang CX. Nonisothermal kinetic analysis of the effect of protein concentration on BSA aggregation at high concentration by DSC. Thermochim Acta. 2008;467:99–106.
27. Cao XM, Yang X, Shi JY, Liu YW, Wang CX. The effect of glucose on bovine serum albumin denatured aggregation kinetics at high concentration. The master plots method study by DSC. J Therm Anal Calorim. 2008;93:451–8.
28. Cao X, Wang ZY, Yang X, Liu YW, Wang CX. Effect of sucrose on BSA denatured aggregation at high concentration studied by the iso-conversional method and the master plots method. J Therm Anal Calorim. 2009;95:969–76.
29. Militello V, Casarino C, Emanuele A, Giostra A, Pullara F, Leone M. Aggregation kinetics of bovine serum albumin studied by FTIR spectroscopy and light scattering. Biophys Chem. 2004; 107:175–87.
30. Militello V, Vetri V, Leone M. Conformational changes involved in thermal aggregation processes of bovine serum albumin. Biophys Chem. 2003;105:133–41.
31. Hatakeyama T, Quinn FX. Thermal analysis dundamentals and applications to polymer science. 2nd ed. England: Wiley; 1999.

32. Mettler Toledo, Software option of STARe Software, DSC Evaluations 13 convertion determination 13-403 Mettler-Toledo GmbH 1993–2002 ME-709319G Printed in Switzerland, 0209/31. 12.
33. Klibanov AM, Ahern TJ, Oxender DL, Fox CF, editors. Thermal stability of proteins. In: Protein engineering. New York: Alan R. Liss; 1987. p. 213–8.
34. Hoffmann MAM, Roefs SPFM, Verheul M, v Mil PJJM, de Kruif CG. Aggregation of β-lactoglobulin studied by in situ light scattering. J Dairy Res. 1996;63:423–40.
35. Alting AC, Hamer RJ, de Kruif CG, Visschers RW. Formation of disulfide bonds in acid-induced gels of preheated whey protein isolate. J Agric Food Chem. 2000;48:5001–7.
36. Boye JI, Alli I, Ismail AA. Interactions involved in the gelation of bovine serum albumin. J Agric Food Chem. 1996;44:996–1004.
37. Haug IJ, Skar HM, Vegarud GE, Langsrud T, Draget KI. Electrostatic effects on β-lactoglobulin transitions during heat denaturation as studied by differential scanning calorimetry. Food Hydrocolloids. 2009;23:2287–93.
38. Ma CY, Harwalkar VR. Effects of medium and chemical modification on thermal characteristics of beta-lactoglobulin. J Therm Anal Calorim. 1996;47:1513–25.
39. Li-Chana ECY, Mab CY. Thermal analysis of flaxseed (*Linum usitatissimum*) proteins by differential scanning calorimetry. Food Chem. 2002;77:495–502.
40. Hédoux A, Willart JF, Ionov R, Affouard F, Guinet Y, Paccou L, et al. Analysis of sugar bioprotective mechanisms on the thermal denaturation of lysozyme from raman scattering and differential scanning calorimetry investigations. J Phys Chem B. 2006;110:22886–93.
41. Makhatadze GI, Privalov PL. Protein interactions with urea and guanidinium chloride: a calorimetric study. J Mol Biol. 1992;226:491–505.
42. Sachurfu, Luo LF, Li QZ. Research on urea-induced protein denaturation. Acta Scientiarum Natura Univ NeiMongo. 2004;35:183–90.
43. Jain S, Ahluwalia JC. Differential scanning calorimetric ammonium and tetraalkylammonium lysozyme studies on the effect of halides on the stability of lysozyme. Biophys Chem. 1996;59:171–7.
44. Mohamed AA, Duarte PR, Kim S. Effect of starch on the thermal kinetics and transmittance properties of lysozyme. J Sci Food Agric. 2005;85:450–8.
45. Hoffmann MAM, van Miltenburg JC, van der Eerden JP, van Mil PJJM, de Kruif CG. Isothermal and scanning calorimetry measurements on β-lactoglobulin. J Phys Chem B. 1997;101:6988–94.
46. Stirpe A, Guzzi R, Wijma H, Verbeet MPh, Canters GW, Sportelli L. Calorimetric and spectroscopic investigations of the thermal denaturation of wild type nitrite reductase. Biochim Biophys Acta. 2005;1752:47–55.
47. Chen YL, Mao HB, Zhang XF, Gong YD, Zhao NM. Thermal conformational changes of bovine fibrinogen by differential scanning calorimetry and circular dichroism. Int J Biol Macromol. 1999;26:129–34.
48. Lyubarev AE, Kurganov BI, Orlov VN, Zhou HM. Two-state irreversible thermal denaturation of muscle creatine kinase. Biophys Chem. 1999;79:199–204.
49. Bon CL, Nicolai T, Durand D. Kinetics of aggregation and gelation of globular proteins after heat-Induced denaturation. Macromolecules. 1999;32:6120–7.
50. Jaenicke R. Folding and association of proteins. Prog Biophys Mol Biol. 1987;49:117–237.